Dear reviewer,

The authors would like to express their sincere gratitude to the reviewer for the comments. These comments are all valuable and helpful for improving our manuscript. Every comment or suggestion was checked very carefully. Based on these comments, we revised the manuscript thoroughly and seriously, which we hope could meet with approval. Point-by-point replies and corresponding modifications are listed in the following.

General Comments:

1. The paper fails to investigate local meteorological and synoptic conditions associated with the case of the sandstorm studied herein. This investigation is crucial as weather features are expected to directly impact large and very large-scale motions (LSMs and VLSMs) of turbulence. Specifically:

1.1. The sandstorm event studied here must be described in details in Section 2.1, including the date/time, weather conditions, potential meteorological drivers, etc (see for example Gasch et al., 2017). Without this information, all the discussion of results regarding the onset of the sandstorm and the link between LSMs/VLSMs and synoptic conditions is questionable.

Reply 1.1:

Thanks for the reviewer's suggestion, it is very valuable. According to the reviewer's suggestion, the authors have perused the detailed description of the sandstorm process in Gasch et al. (2017). The date/time, weather conditions, potential meteorological drivers of the sandstorm have been added in Section 2.1 in the revised manuscript, i.e.,

"From April 16 to 17, 2016 a severe sandstorm occurred in the observation field. The QLOA captured the sandstorm event and obtained high-quality data during the complete process. The sandstorm started at 13:00 local time on the 16th and ended at 03:00 on the 17th, and lasted for 14 hours, as shown in Fig. 2. The streamwise velocity at 5 m shown in Fig. 2(a) indicates that this sandstorm exhibits obvious rising, steady and declining stages. The duration of these three stages is approximately 5 hours, 7 hours and 2 hours, respectively. At the steady stage, the average wind velocity was 11.26 m/s and the instantaneous maximum wind velocity reached up to 22.3 m/s. With the development of the sandstorm, the instantaneous PM10 concentration can reach up to 5.45 mg/m^3, as shown in Fig. 2(c). Given the PM10 percentage in the QLOA site of approximately 2.5%, the total sand concentration may reach up to 218.00 mg/m^3, and the visibility is less than 300 m. In addition, Fig. 2(d) shows that as the sandstorm evolves, the ambient temperature drops sharply about 2 hours after the start of the sandstorm, this is a typical feature of sandstorms induced by a cold front transit (Dragani, 1999; Zhao et al., 2020).

To clarify the cause of the sandstorm, the weather conditions and potential meteorological drivers were also investigated. From April 16 to 17, 2016, the average circulation in mid-high latitudes of Eurasia turned into two troughs and one ridge. The mid-high latitudes from the Ural Mountains to Lake Balkhash were broad ridges, and northern Europe and the vicinity of the Okhotsk Sea were controlled by low-value systems, respectively. From the daily circulation evolution, affected by the westerly trough, plateau trough and south branch trough, surface cyclones moved eastward and developed in Northwest China from April 14 to 16. There was a cold air process with a low trough moving eastward from April 16 to 17. Decreasing temperature occurred in the eastern part of Northwest China, accompanied by 4-6 northerly winds and 7-8 gusts. At the same time, under the influence of the ground cold front and the Mongolian cyclone, sandstorms occurred locally in Northwest and North China."

Please see lines 97–115 on page 4 in the revised manuscript for detailed information.

1.2. Throughout the text, authors referred to the study by He at al. (2020) to describe the physics and meteorological drivers of a sandstorm. This is problematic, because He et al. (2020) investigated a mesoscale convective dust storm generated by cold pool outflow (AKA haboob), which is drastically different that a synoptic-scale dust storm. (see Knippertz (2014) for more information). More concerning is that the paper describes 'synoptic events' and 'cold front' in a sandstorm on the basis of the study of

He et al. (2020), who looked into a haboob sandstorm.

Reply 1.2:

Thanks for the reviewer's comment. The comment is very valuable and helpful for improving our manuscript. Accordingly, the description and corresponding citations describing the physical and meteorological drivers of the sandstorm are comprehensively revised in the manuscript, which are listed as follow:

1. In line 252, the citation is changed to Dragani (1999), i.e., "During the beginning of a sandstorm, the cold air would sink close to the ground (Dragani, 1999; Helfer and Nuijens, 2021)…".

2. In lines 313–314 on page 14 in the original manuscript, the sentence "…that is, the quick dissipation of local sandstorm energy would occur due to interactions of sand-air two-phase flows with the action of vortices (He et al., 2020)…" has been removed.

3. In lines 274-276 on page 11, the sentence "When the cold air reaches the surface, the flat layer of the cold air mass will expand horizontally (He et al., 2020), the coherent structure may be stretched by the horizontal expansion process which could cause the reduced variation of near surface turbulence scale with height." has been changed to "With the intrusion of cold air, the sandstorm begins and the wind velocity starts to increase. The VLSMs are generated by the breaking process of synoptic-scale structures. As the wind velocity increases, the shearing breaking is enhanced, resulting in the reduced scale of the near-surface structures."

4. In line 314 on page 13, the citation is changed to Conrick et al. (2016), i.e., "Moreover, the cold air mass transfers energy to the local atmosphere (Conrick et al., 2016)…".

5. In line 352 on page 15, the sentence "After the intrusion of a cold air into the upper region of the surface convective mixing layer, the cold air descending would lead to the downward transport of vorticity, enabling thermal convection cells in the mixing layer to become swirling convection cells and after development, there occurs many subvortices (He et al., 2020)." has been changed to "The intrusion of cold air causes the convection with the local atmosphere.".

6. In lines 458–459 on page 22 in the original manuscript, the sentence "After the intrusion of a cold air into the upper region of the surface convective mixing layer, the cold air descending would lead to the downward transport of vorticity (He et al., 2020)." has been removed.

7. In lines 420–421 on page 19, the sentence "When the cold air reaches the surface, the flat layer of the cold air mass will expand horizontally (He et al., 2020), which may stretch near-surface structures and thus reduce the variation of turbulence scale with height." has been changed to "As the wind velocity increases, the shearing breaking is enhanced, resulting in the reduced scale of the near-surface structures.".

2. The structure of the paper should be improved. Specifically:

2.1. The paper should be shortened:

- Remove Figure 3 or move it to a supplementary information document as it is simply a repetition of the text (lines 162-174).
- Figure 4 and the discussion around it (lines 175 -192) seems to be out of place and should be moved to a supplementary information document.
- The spectral method (section 3) is a well-established approach in the study of turbulence, and the contribution of this work in terms of methodology development is not clear. Therefore, I suggest this section to be shortened and the text to be moved to a supplementary document.

Reply 2.1:

We are very grateful for the reviewer's suggestions. According to the reviewer's suggestions, Fig. 3 was removed, Fig. 4 and the discussion around it, as well as the spectral method (Section 3) have been moved to the supplementary document.

Please see the supplementary document.

2.2. Lines 198 to 213 should be presented earlier in the paper together with the discussion around Figure 2.

Reply 2.2

Thanks for the reviewer's suggestion. According to the reviewer's suggestion, the contents in lines 198 to 213 has been presented earlier in the revised manuscript and together with the discussion around Figure 2, i.e.,

"The friction Reynolds number ($Re_\tau = u_\tau\delta/\nu$, where u_τ is the friction velocity, δ is the thickness of the ASL and ν is kinematic viscosity) in the steady stage of the sandstorm is approximately 4.5×10^6. The friction velocity u_τ was estimated by eddy covariance ($u_\tau=(-uw)^{1/2}$, u and w are the streamwise and vertical velocity fluctuations, respectively) and averaging at three heights below 2.5 m. The air kinematic viscosity ν was calculated based on the barometric pressure and temperature during the observation. The ASL thickness δ was estimated by the horizontal wind velocity signal (>30 m) collected by Doppler Lidar and was basically kept within the range of 142±23 m for different sandstorm events at the QLOA site. Following the previous work Wang et al. (2020), the δ is adopted as 150 m in this study. The thermal stability of the ASL was characterized by the Monin-Obukhov stability parameter,

$$\frac{z}{L} = -\frac{\kappa z g \overline{w\theta}}{\bar{\theta} u_\tau^3}$$

where, z denotes the measurement height, L denotes the Obukhov length, κ= 0.41 is Kármán constant, g is gravitational acceleration, and $\overline{w\theta}$ is the average vertical heat flux which was calculated by averaging the covariance between the vertical wind velocity w and the temperature θ. The resulting z/L during the sandstorm is shown in Fig. 2(d), where the shaded area marks the near-neutral stratification condition of $|z/L| < 0.1$ (Hogstrom, 1988; Metzger et al., 2010). It is seen that the ASL is basically unstable stratified in the rising stage of the sandstorm, neutrally stratified in the steady stage, and stable stratified in the declining stage."

Please see lines 116–130 on pages 4-5 in the revised manuscript.

Specific Comments

Comment 1: The segmentation method described in figure 3, involves a number of subjective criteria including the IST threshold (30%), the time window used for initial time-averaging (1 hr), and dt (5 min). The uncertainty of these choices in final results should be studied and discussed. Specifically, after applying the data processing procedure the size of all segments ended up being very close to or exactly 1-hr which was the initial choice for time-averaging and removing the time-varying mean. One may ask whether the 1-hr initial choice could basically govern the whole procedure and making the entire segmentation algorithm irrelevant. A sensitivity test should help answering this question.

Reply 1:

Thanks for the reviewer's comment. Point-by-point replies are listed in the following.

The selection of the IST threshold (30%) is based on the work of Foken et al. (2004). They proposed this threshold (30%) by long experience and is in a good agreement with other test parameters also of other authors (Foken and Wichura, 1996). Many subsequent studies have followed this criterion, such as Mauder et al. (2006), Wang and Zheng (2016), Zheng et al. (2015), Han et al. (2019); Liu et al. (2021). In reality, the exact choice of the threshold affects the time size of each segment. For example, the size of the second segment varies from 55 min to 80 min when the IST threshold varies from 20% to 40%. To discuss the uncertainty of these choices in final results, the pre-multiplied spectra of the streamwise velocity fluctuations versus the streamwise wavenumber at different sizes of the second segment are shown in Figure R1 as an example. The general form of the spectra results are seen to remain nominally the same and are thus only weakly dependent on the chosen IST threshold. The maximum standard deviations of 7.5%, 11.4%, 10.2%, 8.6% are within experimental error for these ASL data (Metzger and Klewicki, 2001; Kunkel and Marusic, 2006; Liu et al., 2017).

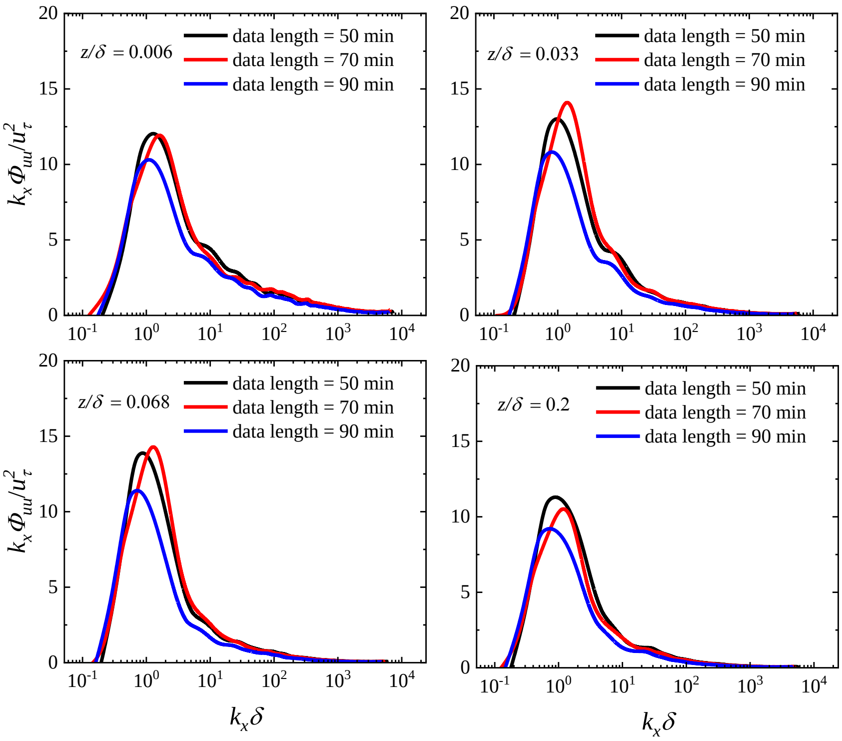

Figure R1. The pre-multiplied spectra of the streamwise velocity fluctuations versus the streamwise wavenumber at different sizes of the second segment.

The standard practice in the study of ASL experimental data suggests that the time scales on the order of 1 hour or less are considered as turbulence while the slower fluctuations as part of the mean field (Wyngaard, 1992). Moreover, the streamwise advection length should be $O(100)$ surface layer thickness to obtain converged statistics (Hutchins et al., 2012), which corresponds to 50 min for the wind speed of 5 m/s and would be smaller for higher wind velocities. Further verification using ogive analysis for time series with the lengths of 20, 30, 40, 50, 55, and 60 min indicates that there is a good collapse in the cumulative frequency distribution for time series with the length more than 50 min, as shown in Figure R2. Therefore, the time window used for initial time-averaging was adopted as 1 hour. Following the reviewer's suggestion, a sensitivity test of the time window used for initial time-averaging is performed, as shown in Figure R3. It is seen that the variation in the size of segments due to the time window used for initial time-averaging is within the range in Figure R1, and thus the final results are only weakly dependent on the chosen the time window used for initial time-averaging.

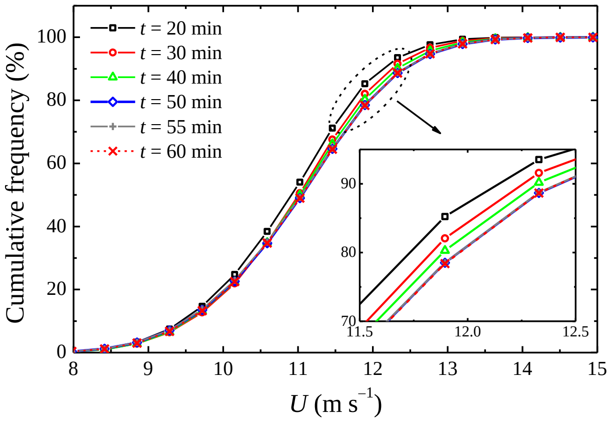

Figure. R2. Cumulative frequency of the time series for streamwise velocity at z = 5 m in the steady stage.

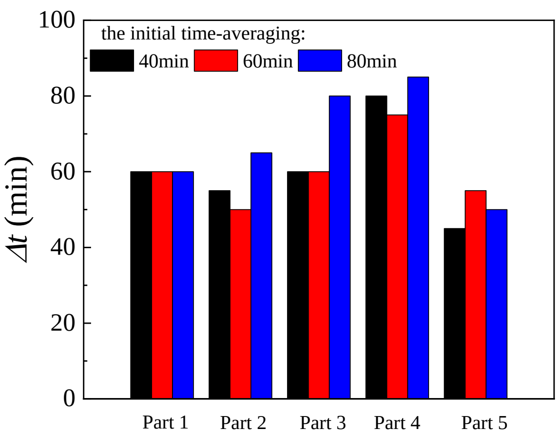

Figure R3. The size of segments for different time windows used for initial time-averaging.

The period of time Δt is determined from the advection times of the energetic turbulence structures dominated in the outer region of the wall-bounded turbulence. The results of Hutchins and Marusic (2007) and Hutchins et al. (2012) suggested that the VLSMs in ASL can reach up to 10δ. The boundary-layer thickness in ASL is approximately 150 m and the typical convection velocity is 5 m/s–20 m/s. This yields the advection times of approximately 1.25–5 min. Hence, the Δt is adopted as 5 min to contain at least a VLSM. The same time interval was also used by other studies, such as Foken et al. (2004), Wang and Zheng (2016), Liu et al. (2019a). Following the reviewer's suggestion, a sensitivity test of Δt is conducted, as shown in Figure R4. It is seen that the variation in the size of segments due to Δt is relatively small, and thus the final results also weakly dependent on the choice of Δt.

In summary, the sensitivity tests of the IST threshold, the time window used for initial time-averaging and Δt indicate that they do not significantly affect the results and conclusions in the present work.

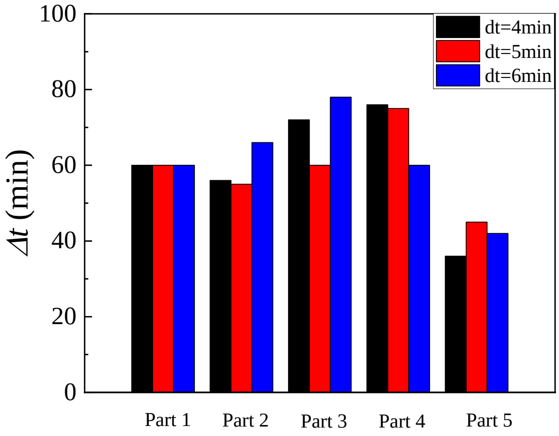

Figure R4. The size of segments for different Δt.

The corresponding elaborations have been added in the revised manuscript, i.e.,

"The period of time Δt is determined from the advection times of the energetic turbulence motions (VLSMs) to contain the dominated structures in the outer region of the wall-bounded turbulence. The results of Hutchins and Marusic (2007) suggested that the VLSMs in turbulent boundary layers can reach up to 10δ, with the δ of 150 m and the convection velocity of 5 m/s–20 m/s, such VLSMs could have advection times of *O*(1.25–5min). Thus, the Δt is adopted as 5 min to be consistent with Foken et al. (2004)." Please see lines 146–151 on page 7 in the revised manuscript for detailed information.

"The sensitivity tests of the IST threshold, the time window used for initial time-averaging and Δt indicate that they do not significantly affect the results and conclusions in the present work." Please see lines 206–207 on page 9 in the revised manuscript for detailed information.

Comment 2： Figure 2(a): Can authors comment why the time-varying average velocity obtained by the EMD method contains low frequency fluctuations in the rising stage, which are absent in the other two methods (moving windows and adaptive wavelet transform)?

Reply 2:

Thanks for the reviewer's comment. For a multicomponent signal $x(t)$, the EMD can decompose it into several intrinsic modal functions (IMFs) and a residual term (Huang et al,, 1998), i.e.,

$$x(t)=\sum_{i=1}^{n}c_i(t)+r_n(t), \tag{1}$$

where $c_i(t)$ is the IMF and $r_n(t)$ is the residual term which represents the overall trend of the signal. With the increase of the order (i) of the IMFs, the center frequency decreases sequentially.

The adaptive wavelet transform can also decompose the $x(t)$ into a series of successive octave band components (Percival and Walden, 2000) as follows:

$$x(t)=\sum_{i=1}^{n}\psi_i(t)+\chi_n(t), \tag{2}$$

where n is the total number of decomposition levels, $\psi_i(t)$ denotes the ith level wavelet detail component (high frequency), and $\chi_n(t)$ represents the nth level wavelet approximation component (low frequency). As n increases, the frequency contents become lower, and thus, the nth level approximation components could be regarded as the time-varying mean values (e.g. Percival and Walden, 2000; Su et al., 2015).

In the EMD method, the frequency of the 23-order IMF ($c_{23}(t)$) is 3.15×10^{-4} Hz and the 24-order IMF ($c_{24}(t)$) is 1.69×10^{-4} Hz. The frequency of 23-order IMF is closer to the 1-hour period (corresponding frequency of 2.78×10^{-4} Hz). Hence, the residual term $r_{23}(t)$ is regarded as the time-varying average velocity. However, for adaptive wavelet transform, the 18th level wavelet detail component ($\psi_{18}(t)$) with the frequency of 1.91×10^{-4} Hz is closer to the 1-hour period. Thus, the $\chi_{18}(t)$ is regarded as the time-varying average velocity. As for the moving windows, the size of the windows is selected as 1 hour, which only retains the fluctuations with period larger than 1 hour. Therefore, the time-varying average velocity obtained by the EMD method contains more high frequency fluctuations, which are absent in the other two methods.

Comment 3: The studies of Kim and Adrian (1999), Guala et al. (2006), and Balakumar and Adrian (2007) have been referred to throughout the text to describe and identify LSMs/VLSMs. All these studies investigated turbulent channel and pipe flows (internal), rather than a true turbulent boundary layer flow as relevant to a sandstorm (external). Monty et al. (2009) concluded that VSLMs in boundary layers are different from those in channel and pipe flows (e.g., as in Kim and Adrian (1999)). Therefore, there is a concern in using results/criteria from internal flows in the case of a sandstorm with very high Reynolds number.

Reply 3:

Thanks for the reviewer's comment. The authors carefully checked every citation to these works.

1. "The VLSMs are associated with the wavelengths of the lower wavenumber peaks in the pre-multiplied spectra of the streamwise velocity fluctuations (Kim and Adrian, 1999)." This is the same as that in the turbulent boundary layer, such as, Vallikiv et al., (2015). The corresponding citation has been changed to Vallikiv et al., (2015) in the revised manuscript. Please see line 216 on page 9 in the revised manuscript for detailed information.

2. "The calculation of the pre-multiplied spectrum follows the methods of Kim and Adrian (1999) and Kunkel and Marusic (2006)." The spectral method is a universal mathematical tool for different types of flow.

3. "The decrease in $k_x\Phi_{uu}$ with height in the high wavenumber region is consistent with the "bottom-up" mechanism proposed by Kim and Adrian (1999);". Adrian et al. (2000) also described this mechanism in boundary layer flow. The authors have added a reference to Adrian et al. (2000) in the revised manuscript. Please see line 236 on page 9 in the revised manuscript for detailed information.

4. "that is, the small-scale structures originate from the self-organization process of hairpin vortices (or a quasi-streamwise vortex) near the wall (Kim and Adrian,

1999).” The citation here has been changed to Dennis (2015), which is a review of the coherent structure. Please see line 388 on page 16 in the revised manuscript for detailed information.

5. “According to Guala et al. (2006) and Balakumar and Adrian (2007), coherent structures with streamwise scales larger than 3δ (corresponding $k_x\delta < 2\pi/3$) are VLSMs.” and “Since LSMs/VLSMs (with streamwise length scales larger than 0.1πδ nominally (Guala et al., 2006; Balakumar and Adrian, 2007))”. The study in Balakumar and Adrian (2007) included both channel flow and boundary layer flow. Moreover, this standard is also used in the subsequent studies in the boundary layer flow, such as, Dennis and Nickels (2011), Heisel et al. (2018), Barros and Christensen (2019), Gibeau and Ghaemi (2021), and Chan et al. (2021), In the revised manuscript, the reference to Guala et al. (2006) is changed to Heisel et al. (2018). Please see line 226 on page 9 in the revised manuscript for detailed information.

Comment 4： Figure 6: What is the difference between subfigures (a) and (b), (c) and (d), (e) and (f)? It was neither mentioned in the caption nor discussed in the main text.

Reply 4：

Thanks for the reviewer’s comment. Subfigures (a) and (b), (c) and (d), (e) and (f) of Figure 6 represent the result of the same stage of the sandstorm to ensure that the phenomenon in different stages are universal. For brevity, only one subfigure remains for each stage of the sandstorm in the revised manuscript, as shown in Figure R5.

Please see Figure 3 on page 11 in the revised manuscript.

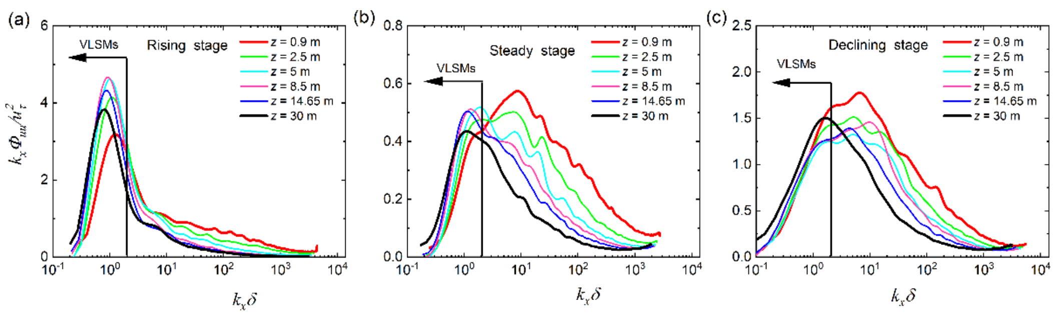

Figure R5. Pre-multiplied spectra of streamwise velocity fluctuations $k_x\Phi_{uu}/u_\tau^2$ versus streamwise wavenumber $k_x\delta$, where (a) are the rising stage, (b) are the steady stage, and (c) are the declining stage.

Comment 5: Figure 7(b) and lines 330-333: The sharp decreases in the declining stage were attributed to the exhaustion of energy at this stage, but why there is a maximum right when the declining stage is started and before this sharp decrease?

Reply 5:

Thanks for the reviewer's comment. The analysis of the pre-multiplied spectra (as shown in Figure 3) indicates that the "top-down" process exists in the entire sandstorm process, that is, the large synoptic-scale structures in the outer region of the turbulent boundary layer moves downwards accompanied by breaking into smaller structures due to quadratic phase coupling, which is detailed in sub-section 3.2. In the late the steady stage (before the start of the declining stage), the average wind velocity remains constant (as shown in Fig. 2a), which indicates that the synoptic-scale fluctuations determined by the mean flow are approximately invariant (Hutchins et al. 2012). However, the quadratic phase coupling weakens in the late the steady stage (as shown in Fig. 7 in the revised manuscript), suggesting a weakened breaking of the synoptic-scale structures. This leads to the increase of the scale of the near-surface flow structures. During the declining stage, the energy brought by the cold air mass is exhausted, leading to the reduced wind velocity, and thus the flow is difficult to maintain, which is represented by a reduction in flow structure. Therefore, there is a maximum right when the declining stage is started and before this sharp decrease.

The corresponding elaboration has been added in the revised manuscript, i.e.,

"In addition, Fig. 4(b) shows a maximum right when the declining stage is started and before this sharp decrease. A plausible explanation for the increase of the scale of the near-surface flow structures is the weakened breaking of the synoptic-scale structures due to the attenuated quadratic phase coupling. In the late of the steady stage (before the start of the declining stage), the average wind velocity remains constant (as shown in Fig. 2a), which indicates that the synoptic-scale fluctuations determined by the mean flow is approximately invariant (Hutchins et al. 2012). However, the quadratic phase coupling weakens in the late of the steady stage (as shown in Fig. 7), suggesting a weakened breaking of the synoptic-scale structures.”

Please see lines 281–287 on page 11 in the revised manuscript for detailed information.

Comment 6: Figure 8: The two fraction numbers contributed by VLSMs of 75% and 40% reported throughout the text were obtained from this figure. As this fraction is changing with height, it is crucial that either the location where the fraction is reported be mentioned everywhere in the text or an average value below a certain height be reported. It seems that the two reported fraction values (75% and 40%) are simply the limit of measurements in terms of height.

Reply 6:

Thanks for the reviewer’s suggestion, this suggestion is helpful for improving the rigor of our manuscript. The two reported fraction values are the results at the highest position (z/δ = 0.2) in the present ASL observation. The location where the fraction is reported has been mentioned everywhere in the text, i.e.,

Line 6: “… streamwise kinetic energy of 75% (at z/δ = 0.2) rather than…”

Line 9: “… energy fraction reducing to 40% (at z/δ = 0.2) in the declining stage…”

Line 292: “…reach up to 75% at the highest position (z/δ = 0.2) in the present ASL observation…”

Lines 293-294: “…which only reaches up to 60% at z/δ = 0.2…”

Line 295: “…approximately 40% of the total energy at z/δ = 0.2.”

Line 444: “…reach up to 75% (at z/δ = 0.2)…”

Line 456: “…only approximately 40% (at z/δ = 0.2) of the total kinetic energy…”

Comment 7: The Taylor’s hypothesis of frozen turbulence has been used throughout the text. Does the level of turbulence intensity (i.e., fluctuations compared to the mean wind value) justify this approximation?

Reply 7:

Thanks for the reviewer's comment. Lin (1953) pointed out that the Taylor's hypothesis is applicable when the turbulence intensity ($\sqrt{\overline{uu}}/\overline{U}$) is less than 0.1. Figure R6 shows the turbulence intensity at different heights during the entire sandstorm process. It is seen in Figure R6 that the turbulence intensity is approximately less than 0.1 except for the position closest to the ground and the beginning of the sandstorm (the first segment). Therefore, the Taylor's hypothesis can be considered to be approximately applicable in this study. The corresponding elaboration has been added in the revised manuscript, i.e.,

"The level of turbulence intensity (i.e., fluctuations compared to the mean wind value) is less than 0.1 at most of the position in the entire sandstorm process, which justify the approximation of the Taylor's hypothesis (Lin, 1953)."

Please see lines 344-346 on page 15 in the revised manuscript.

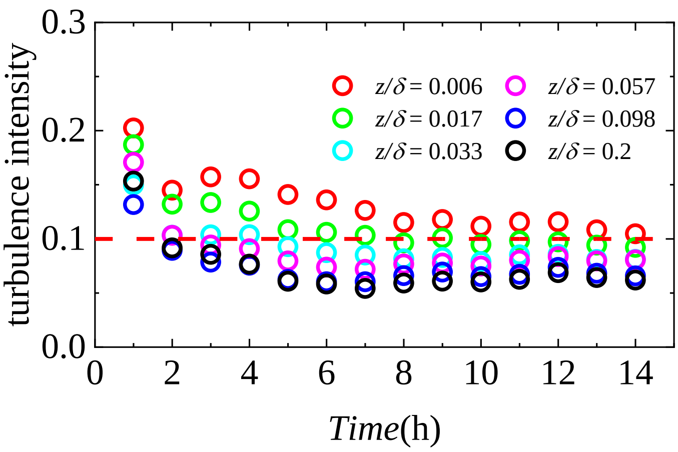

Figure R6. Variation of turbulence intensity with time at different heights.

Comment 8: Figure 11 and the text around it: How are the "small-scale motions" defined? (This point may be linked to point 3 above questioning the criteria to define VLSMs).

Reply 8:

Thanks for the reviewer's comment. According to the definition in the turbulent boundary layer (Balakumar and Adrian 2007; Dogan et al., 2019) and the ASL (Wang and Zheng, 2016; Liu et al., 2019a), the turbulent motions with the streamwise length scales shorter than $0.1\pi\delta$ are termed small-scale motions. The corresponding definition is given in the caption of Figure 8, i.e., "(d-f) Evolution of the total integral bispectra for small-scale motions (λ < 0.3δ, Wang and Zheng, 2016) at different heights, …".

Please see the caption in Fig. 8 on page 17 in the revised manuscript.

Comment 9: Figure 11: Including an inset in (b) and (c) are quite confusing. I think the plots for all the heights can be presented as the main figure instead of being included as an inset.

Reply 9:

We are very grateful for the reviewer's suggestion. According to the reviewer's suggestion, the authors have revised the figure to use the plots for all the heights as the main figure instead of being included as an inset, as shown in Figure R7. Please see Figure 8 on page 17 in the revised manuscript.

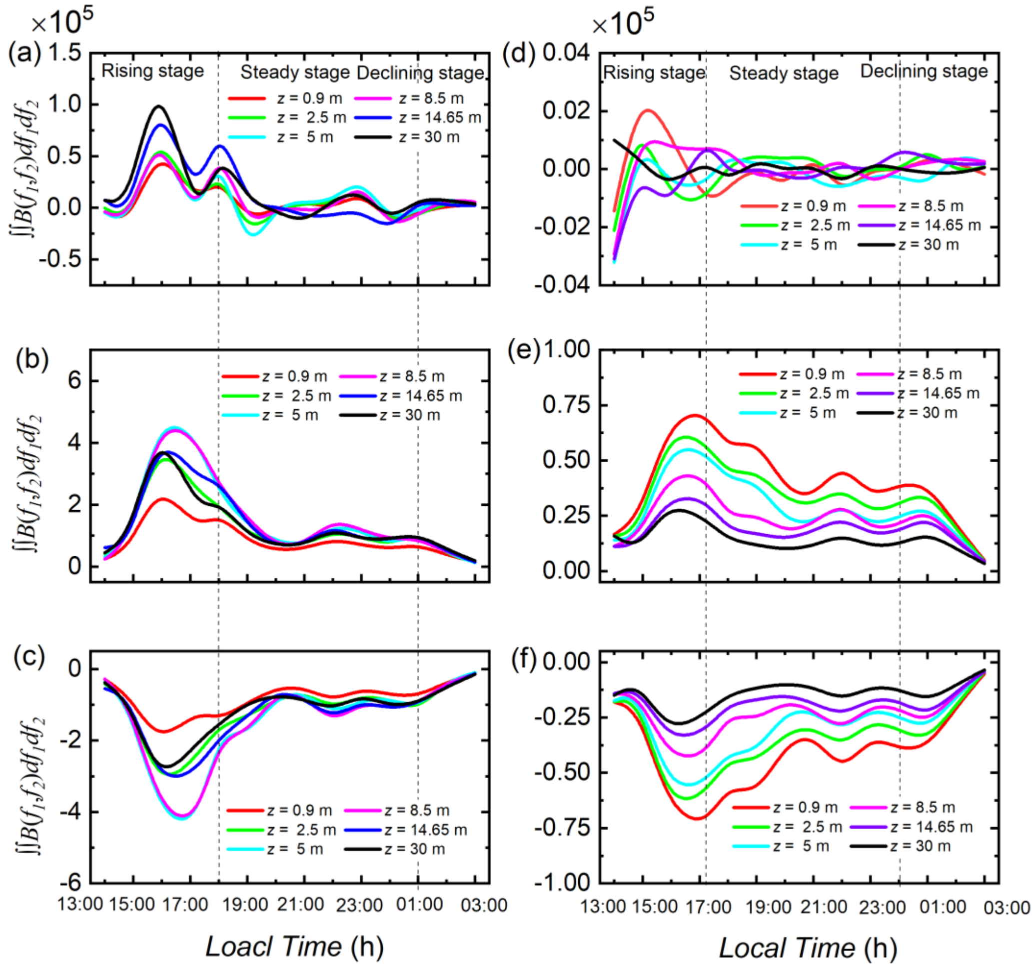

Figure R7. Evolution of the total integral bispectra. (a-c) Evolution of the total integral bispectra for LSMs/VLSMs at different heights, (a) the overall bispectra integrals, (b) positive and (c) negative bispectra integrals. (d-f) Evolution of the total integral bispectra for small-scale motions ($\lambda < 0.3\delta$) at different heights, where the settings of (d)-(f) are similar to those of (a)-(c).

Comment 10： Line 481-486: This statement seems to be an overgeneralization of the lifetime of a sandstorm based on observations of a single event (This point is directly linked to my first point under general comments).

Reply 10：

Thanks for the reviewer's comment. According to the reviewer's comment, the authors have removed the statement in lines 481-486.

Comment 11： The data provided in the Zenodo data repository has no metadata, data header, or any information to help using this data.

Reply 11:

Thanks for the reviewer's comment. According to the comment, the authors have re-uploaded the data and supplemented information to help using this data, which can be available at https://zenodo.org/record/6459518.

Technical Comments:

Comment 1: Line 14: check for grammar correction

Reply 1:

Thanks for the reviewer's suggestion. According to the suggestion, the grammar has been corrected, "Analyzing the temporal and spatial characteristics and the causes of sandstorms can help us better understanding their occurrence and development, improving the level of sandstorm forecasting, and reducing disaster impact and loss."

Please see lines 14–16 on page 1 in the revised manuscript.

Comment 2: Line 19: use "humidity" instead of "dampness"

Reply 2:

We are very grateful for the reviewer's suggestion. The authors have used "humidity" instead of "dampness" in line 19 on page 1 in the revised manuscript.

Comment 3: Line 24: "A kind of power": sounds awkward

Reply 3:

Thanks for the reviewer's comment. The corresponding sentence has been modified, "However, wind, as a driving force, is the energy source of wind-blown sand movement."

Please see lines 24–25 on page 1 in the revised manuscript.

Comment 4: Line 27: "… impact on sandstorm more intensively, significantly, contributively than other…" : sounds awkward

Reply 4:

Thanks for the reviewer's comment. The corresponding sentence has been modified as: "… have a more significant impact on sandstorm than other…"

Please see lines 26–27 on page 2 in the revised manuscript.

Comment 5： Line 49 and throughout the text: use "transport" instead of "transportation"

Reply 5:

Thanks for the reviewer's suggestion. The authors have used "transport" instead of "transportation" throughout the text in the revised manuscript, i.e.,

Line 48: "…the streamwise transport of sand particles…"

Line 255: "…with the momentum transport downward…"

Line 259: "…affected by the momentum transport downward…"

Line 261: "…and the momentum transport downward are weakened…"

Line 354: "…wind velocity is the momentum transport downward…"

Line 424: "…With the momentum transport downward…"

Line 426: "…and the momentum transport downward make the energy fraction…"

Comment 6： Line 85: "necessary": Do you mean "ideal" or "suitable" ?

Reply 6:

Thanks for the reviewer's comment. The authors have revised the corresponding sentence, "This area …, and is on the path of cold air traveling northwest through China."

Please see lines 83–84 on page 3 in the revised manuscript.

Comment 7： Throughout the text: I suggest using "surface" instead of "wall". I understand that "wall-bounded turbulence" is an established term, but the word "surface" or "ground" seems to better suit an atmospheric application.

Reply 7:

We are very grateful for the reviewer's suggestion. According to the reviewer's suggestion, the authors have used “surface” instead of “wall” throughout the text in the revised manuscript.

Please lines 242,302,313,362,399 and 414 in the revised manuscript for detailed information.

References

Adrian, R. J., Meinhart, C. D., & Tomkins, C. D., 2000. Vortex organization in the outer region of the turbulent boundary layer. *Journal of Fluid Mechanics*, 422, 1-54.

Balakumar, B. J., & Adrian, R. J., 2007. Large- and very-large-scale motions in channel and boundary-layer flows. *Philosophical Transactions of the Royal Society a-Mathematical Physical and Engineering Sciences, 365*(1852), 665-681.

Barros, J. M., & Christensen, K. T., 2019. Characteristics of large-scale and superstructure motions in a turbulent boundary layer overlying complex roughness. *Journal of Turbulence, 20*(2), 147-173.

Chan, C. I., Schlatter, P., & Chin, R. C., 2021. Interscale transport mechanisms in turbulent boundary layers. *Journal of Fluid Mechanics, 921*.

Conrick, R., Curtis, N. L., Staten, P. W., and Kirkpatrick, C., 2016. The relationships between temperature gradient and wind during cold frontal passages in the eastern United States: a numerical modeling study. *Atmospheric Science Letters*, 17, 339–345.

Dennis, D. J. C., & Nickels, T. B., 2011. Experimental measurement of large-scale three-dimensional structures in a turbulent boundary layer. Part 2. Long structures. *Journal of Fluid Mechanics, 673*, 218-244.

Dennis, D. J. C., 2015. Coherent structures in wall-bounded turbulence. *Anais da Academia Brasileira de Ciências, 87*(2), 1161-1193.

Dogan, E., Hearst, R. J., Hanson, R. E., & Ganapathisubramani, B., 2019. Spatial characteristics of a zero-pressure-gradient turbulent boundary layer in the presence of free-stream turbulence. *Physical Review Fluids*, 4(8).

Dragani, W. C., 1999. A feature model of surface pressure and wind fields associated with the passage of atmospheric cold fronts. *Comput Geosci*, 25, 1149–1157.

Foken, T. , and B. Wichura., 1996. Tools for quality assessment of surface-based flux measurements. *Agricultural & Forest Meteorology*, 78.1-2:83-105.

Foken, T et al., Post-Field Data Quality Control. X. Lee, W. Massman, B. Law, Eds., Handbook of Micrometeorology: A Guide for Surface Flux Measurement and Analysis (Springer Netherlands, Dordrecht, 2004), pp. 181-208.

Gasch, P., Rieger, D., Walter, C., Khain, P., Levi, Y., Knippertz, P. and Vogel, B., 2017. Revealing the meteorological drivers of the September 2015 severe dust event in the Eastern Mediterranean. *Atmospheric Chemistry and Physics*, 17(22), pp.13573-13604.

Gibeau, B., & Ghaemi, S. 2021. Low- and mid-frequency wall-pressure sources in a turbulent boundary layer. *Journal of Fluid Mechanics, 918*, 45.

Guala, M., Hommema, S. E., & Adrian, R. J., 2006. Large-scale and very-large-scale motions in turbulent pipe flow. *Journal of Fluid Mechanics, 554*, 521-542.

Han, G., Wang, G., & Zheng, X., 2019. Applicability of Taylor's Hypothesis for Estimating the Mean Streamwise Length Scale of Large-Scale Structures in the Near-Neutral Atmospheric Surface Layer. *Boundary-Layer Meteorology*, 172(2), 215-237.

Heisel, M., Dasari, T., Liu, Y., Hong, J., Coletti, F., & Guala, M., 2018. The spatial structure of the logarithmic region in very-high-Reynolds-number rough wall turbulent boundary layers. *Journal of Fluid Mechanics, 857*, 704-747.

Hogstrom, U., 1988. Non-dimensional wind and temperature profiles in the atmospheric surface-layer-a re-evaluation. *Bound-Lay Meteorol*, 42, 55–78.

Huang, N. E., Shen, Z., Long, S. R., Wu, M. L. C., Shih, H. H., Zheng, Q. N., Liu, H. H., 1998. The empirical mode decomposition and the Hilbert spectrum for nonlinear and non-stationary time series analysis. *Proceedings of the Royal Society a-Mathematical Physical and Engineering Sciences*, 454(1971), 903-995.

Hutchins, N., & Marusic, I., 2007. Evidence of very long meandering features in the logarithmic region of turbulent boundary layers. *Journal of Fluid Mechanics*, 579, 1-28.

Hutchins, N., Chauhan, K., Marusic, I., Monty, J., and Klewicki, J., 2012. Towards Reconciling the Large-Scale Structure of Turbulent Boundary Layers in the Atmosphere and Laboratory. *Bound-Lay Meteorol*, 145, 273–306.

Kim, K. C., & Adrian, R. J., 1999. Very large-scale motion in the outer layer. *Physics of Fluids, 11*(2), 417-422.

Kunkel, G. J., & Marusic, I., 2006. Study of the near-wall-turbulent region of the high-Reynolds-number boundary layer using an atmospheric flow. *Journal of Fluid Mechanics*, 548, 375-402.

Li, X. L. and Zhang, H. S., 2021. Seasonal variations in dust concentration and dust emission observed over Horqin Sandy Land area in China from December 2010 to November 2011. *Atmos Environ*, 61, 56–65.

Lin, C. C., 1953. On Taylor's hypothesis and the acceleration terms in the Navier-Stokes equation, Quarterly of Applied Mathematics, 10, 295–306,560.

Liu, H., Wang, G., & Zheng, X., 2019a. Amplitude modulation between multi-scale turbulent motions in high-Reynolds-number atmospheric surface layers. *Journal of Fluid Mechanics, 861*, 585-607.

Liu, H., He, X., & Zheng, X., 2021. An investigation of particles effects on wall-normal velocity fluctuations in sand-laden atmospheric surface layer flows. *Physics of Fluids*, 33(10).

Liu, X. L., Yi, S. H., Xu, X. W., Shi, Y., Ouyang, T. C., & Xiong, H. X., 2019b. Experimental study of second-mode wave on a flared cone at Mach 6. *Physics of Fluids*, 31(7).

Mang, H. S., Zhu, H., Peng, Y., Kang, L., Chen, J., and Park, S. U., 2008. Experiment on dust flux during duststorm periods over desert area. *Acta Meteorol Sin*, 22, 239–247.

Mauder, M. et al., 2006. Processing and quality control of flux data during LITFASS-2003. *Bound-Lay Meteorol*, 121, 67-88.

Metzger, M., McKeon, B., and Arce-Larreta, E., 2010. Scaling the characteristic time of the bursting process in the turbulent boundary layer. *Physica D*, 239, 1296–1304.

Percival, D. B. and Walden, A. T.: Wavelet methods for time series analysis, Cambridge, UK, Cambridge UP, 2000.

Su, Y., Huang, G., and Xu, Y. L., 2015 Derivation of time-varying mean for non-stationary downburst winds, *J. Wind Eng. Ind. Aerod*., 141, 39–48.

Vallikivi, M., Ganapathisubramani, B., & Smits, A. J., 2015. Spectral scaling in boundary layers and pipes at very high Reynolds numbers. *Journal of Fluid Mechanics, 771*.

Wang, G., Bo, T., Zhang, J., Zhu, W., & Zheng, X., 2014. Transition region where the large-scale and very large scale motions coexist in atmospheric surface layer: wind tunnel investigation. *Journal of Turbulence*, 15(3), 172-185.

Wang, G., & Zheng, X., 2016. Very large scale motions in the atmospheric surface layer: a field investigation. *Journal of Fluid Mechanics*, 802, 464-489.

Wang, G., Gu, H., and Zheng, X., 2020. Large scale structures of turbulent flows in the atmospheric surface layer with and without sand. *Phys. Fluids*, 32, 106 604.

Wyngaard, J. C., 1992. Atmospheric-turbulence. *Annual Review of Fluid Mechanics, 24*, 205-233.

Zhao, J. H., Long, X., Zhang, F., Yang, Y. L., Liu, S. X., and Yun, L., 2020. The role of turbulent coherent structure in sand-dust emissions in a sand/dust storm of the middle China-Mongolia regime. *Chinese J Geophys-Ch*, 63, 3967–3980.

Zheng, X., Wang, G., Bo, T., & Zhu, W.,2015. Field Observations on the Turbulent Features of the Near-surface Flow Fields and Dust Transport During Dust Storms. *Procedia IUTAM*, 17, 13-19.